Scanning Tunneling Microscopy of Discontinuous Polystyrene Films Adsorbed on Graphite

L. S. Zhang, C. W. Manke,* and K. Y. S. Ng

Department of Chemical Engineering and Materials Science and Institute for Manufacturing Research, Wayne State University, Detroit, Michigan 48202

Received March 17, 1995; Revised Manuscript Received August 4, 1995[⊗]

ABSTRACT: Discontinuous polystyrene thin films adsorbed on graphite surfaces from dilute solutions were imaged directly by scanning tunneling microscopy (STM), without the use of conductive overcoating. Dimensions of the adsorbed PS structures were evaluated by measurement of the STM images. At low surface coverage (<10%), the adsorbed polystyrene structures were found to be thin, flat "micro-islands", which are typically composed of 3−50 polystyrene molecules. Monodisperse polystyrene standards of molecular weights ranging from 7000 to 3 000 000 were used to investigate the effect of molecular weight on the micro-island dimensions. The smallest of the imaged structures were identified as single polymer molecules. These single-chain structures have elongated, asymmetric shapes similar to those predicted by statistical theories. The mean square radius of the single-chain micro-islands was found to vary with molecular weight raised to the exponent 1.24, while the apparent thickness was found to depend only weakly on molecular weight.

Introduction

The behavior of polymers at solid−liquid interfaces is important to technological areas such as films and coatings, lubricants, colloidal dispersions, adhesives, and composite materials. Elucidation of the structure or conformation of polymers at interfaces is often a crucial step toward understanding their behavior. Interest in the small-scale structure of polymers at interfaces has promoted experimental efforts to visualize the shape of polymer molecules deposited on solid surfaces, as well as theoretical investigations of the conformations of such polymers. The theoretical studies include computer simulations of adsorbed chain conformations by methods such as Brownian dynamics[1] and lattice Monte Carlo studies,[2,3] where adsorption is modeled at the molecular level with bead and connector representations of the polymer chain structure. Experimentally, ellipsometry and neutron scattering,[4,5] among other techniques, have been used to study thin polymer films, and the latter method has produced detailed information about polymer segment density profiles at interfaces. Transmission electron microscopy (TEM) has also been used to obtain images of single polymer molecules deposited on surfaces by spraying precipitant-treated polymer solutions.[6−8] In TEM imaging, a metal coating is generally applied, and surface topographical information is obtained indirectly by a "shadow casting" technique.[9] Scanning tunneling microscopy[10] (STM), which profiles small-scale surface structure by means of an electrical tunneling current, has become a very useful technique for imaging the structure of conducting molecules and conducting polymers.

Conventional STM imaging can be extended to nonconducting polymers by applying a conductive film over the polymer structures. Recently, Stange *et al.*[11] have used STM, atomic force microscopy (AFM), and ellipsometry to examine thin films of polystyrene (PS) spin-coated from dilute solutions onto silicon wafers at various PS concentrations. At very low concentrations (about 0.0005 wt %), they found that the spin-coated polystyrene was deposited as small molecular aggregates and individual molecules, which they were able to image by STM, employing a conductive carbon overcoating, and by AFM. The sizes of the imaged PS structures were found to correlate directly with molecular volumes calculated from the bulk density of PS. Under proper conditions, thin nonconducting organic adsorbates, such as polymers, deposited on conductive surfaces can also be imaged directly by STM, thereby eliminating the need for conductive overcoating and accompanying concerns about the effects of overcoating on structural details.

In what follows, STM is employed to investigate the structure of discontinuous PS films deposited from dilute solutions onto highly oriented pyrolytic graphite surfaces. As in the study by Stange *et al.*,[11] we use monodisperse PS solutes of different molecular weights to examine the relationship between the sizes of imaged structures and molecular weight. However, our study primarily investigates the structure of molecular aggregates and molecules deposited by adsorption from quiescent solutions, thereby probing molecular shapes produced by near-equilibrium processes. To preserve details of the shapes of small polymer structures, particularly individual molecules, we image our samples directly, without the use of a conductive overcoating layer. The images produced by this study include discontinuous polymer films remaining after evaporation of dilute polystyrene solutions; molecular aggregates, or "micro-islands", adsorbed from dilute, unentangled PS solutions; and adsorbed structures comparable in size to single polymer molecules. The images of the single adsorbed molecules are rendered in sufficient detail to measure the principal axis and the minor axis of molecular conformations and to measure the molecules' orientations relative to the scanning direction.

Experimental Section

Materials. The polymer adsorbates were atactic polystyrene (PS) molecular weight standards with molecular weights ranging from 7025 to 3 000 000, as detailed in Table 1. These high-purity PS standards, supplied by Waters and Poly-Sciences, are nearly monodisperse (M_w/M_n < 1.12), enabling us to examine the effect of molecular weight on the dimensions

[⊗] Abstract published in *Advance ACS Abstracts,* September 15, 1995.

0024-9297/95/2228-7386$09.00/0

Table 1. Table of Materials

	M_w	M_w/M_n	supplier
polystyrene	7 025	1.04	Waters
	18 100	1.02	Waters
	30 740	1.01	Waters
	64 000	1.01	PolySciences
	106 280	1.02	Waters
	707 000	1.05	Waters
	1 090 000	1.08	PolySciences
	3 000 000	1.12	PolySciences
solvent supplier:	toluene, HPLC grade Johnson Matthey		
substrate supplier:	highly oriented pyrolytic graphite (HOPG) Union Carbide		

Table 2. Solution Concentrations for Both Adsorption and Droplet Evaporation Methods

M_w of PS	$[\eta]$ (dL/g)	C (g/L)[a]	C (mg/L)[b]	α (%)[c]
7 025	0.060	110	0.20	8.6
18 100	0.122	55	0.10	8.7
30 740	0.181	37	0.08	8.3
64 000	0.314	21		7.8
106 280	0.459	15	0.03	7.0
707 000	1.902	3.5		6.7
1 090 000	2.631	2.5		8.3
3 000 000	5.623	1.2		9.1

[a] Concentration used for adsorption deposition. [b] Concentration used for droplet evaporation deposition. [c] Total surface coverage of PS on HOPG from samples prepared by adsorption.

of adsorbed PS structures. The absence of crystallinity, which is associated with the isotactic or syndiotatic isomers of PS, was confirmed by differential scanning calorimetry. Solutions for substrate treatment were prepared by dissolving these PS standards in HPLC grade toluene.

Highly oriented pyrolytic graphite (HOPG), supplied by Union Carbide, was selected as the substrate for adsorption studies because it provides an atomically flat surface with high electrical conductivity to facilitate STM imaging. The hexagonal arrangement of carbon atoms on regions of clean HOPG surface provides an easily recognizable surface topology that contrasts with the surfaces of amorphous polystyrene adsorbates. As with most substrates, STM images of HOPG surfaces can include artifacts caused by defects such as ledges and debris particles.[12-14] However HOPG surfaces have been studied extensively by STM, and most of these artifacts are now well-known, which simplifies the task of distinguishing polymer structures from other surface features.

Sample Preparation. All specimens were prepared by depositing polymer onto HOPG substrates from very dilute solutions of PS in toluene. Two deposition methods were employed: (1) adsorption from solution; and (2) droplet evaporation. The adsorption method was used to produce discontinuous polymer films with low surface coverage (less than 10% by area). In this method, a freshly cleaved HOPG substrate is submerged in PS–toluene solution for at least 24 h to allow equilibrium adsorption (studies of adsorption of PS on charcoal media,[15] a similar substrate, indicate that equilibrium is reached in about 9–10 h). The PS concentrations of the adsorbate solutions are selected so that the coil overlap parameter $c[\eta]$, where c is the PS concentration and $[\eta]$ is intrinsic viscosity, is less than unity, thereby avoiding polymer chain entanglements in the bulk solution. Since $[\eta]$ increases with molecular weight,[16] solution concentrations must be adjusted accordingly, as shown in Table 2. After the adsorption step, the substrates are subjected to a series of brief (<10 min) rinses in fresh HPLC grade toluene to remove any polymer that is not strongly attached to the surface. The polymer structures remaining after solvent rinsing are presumed to be strongly adsorbed molecules. The rinsed samples are dried in a desiccator for at least 24 h and then exposed to air at ambient humidity for at least 12 h prior to STM imaging.

Droplet evaporation was employed to produce discontinuous films of higher surface coverage that could be more easily analyzed to confirm the presence of polystyrene on the surface. In this method, a 10 μL droplet of PS solution is placed directly onto the surface of a freshly cleaved HOPG substrate with a micropipet. The specimen is then air-dried in a desiccator for at least 24 h, whereupon the PS present in the original droplet is left as a residue on the substrate surface. The solution concentrations used for droplet evaporation, given in Table 2, were selected to give about 30% surface coverage of PS. These concentrations are lower than those used for adsorption because all the polymer present in the droplets ultimately deposits on the HOPG surfaces.

STM Imaging. The polystyrene films on HOPG substrates, prepared as described above, were imaged using a Nanoscope II STM (Digital Instruments, Inc.) equipped with scanner A, which has a scanning range of approximately 1000 nm × 1000 nm. Imaging was performed in the constant-current mode at room temperature with the sample exposed to ambient air at relative humidities ranging from 20 to 40%. Mechanically cut Pt–Ir tips, supplied by Digital Instruments, were used at scanning frequencies ranging from 4.3 to 8.7 Hz to produce real-time images with limited thermal drift.

Although STM is most often employed on conductive surfaces, a number of researchers[17-23] have demonstrated that this technique can also be applied to image thin nonconducting layers. Here we have imaged the polymer films directly, without employing any conductive coating, to obtain high resolution of the adsorbed PS and to avoid possible structural alterations that might be introduced by overcoating with a conductive material. Under these circumstances, relatively high tip bias voltages, ranging from −0.3 to −1.5 V, are needed to obtain stable images. Typical tunneling currents range from 0.3 to 1.0 nA. Bias voltage and current are optimized for each image, thus different parameter values are employed for each scanned area. The variability in the conditions required to obtain high image quality is probable due to variations in the thickness and surface coverage of the nonconducting layers. Other aspects of polymer imaging are discussed below.

Results and Discussion

Identification of Polystyrene Structures. Adsorbed structures can be easily distinguished as protrusions above the smooth plane of the graphite surface in large-scale images, and by contrast with the distinctive hexagonal arrangement of carbons on the clean HOPG surface at the atomic level. Among the adsorbed structures, we must distinguish polystyrene structures from artifacts such as graphite debris particles, dust, and other impurities. This was accomplished by (1) comparisons of adsorbed PS structures with specimens with discontinuous PS films, for which the presence of PS could be verified by FTIR; (2) analysis of adsorbed PS structures by scanning tunneling spectroscopy (STS); and (3) correlation of adsorbed PS structure size with molecular weight.

Deposition by droplet evaporation was employed to produce discontinuous PS films with about 30% surface coverage of PS. The morphology of the polymer was examined in areas where the PS film adjoins bare regions of the HOPG surface. Figure 1 shows an STM image taken at the boundary between a polystyrene film deposited by droplet evaporation and a region of clean HOPG surface. The polystyrene structure appears as an irregularly-shaped amorphous cluster protruding above the plane of the HOPG surface. The presence of a PS film on the surface of this specimen was verified by the detection of characteristic FTIR adsorption peaks[24] at 700 cm^{-1} (C–C vibrations in out-of-plane phenyl ring), 2923 cm^{-1} (aliphatic C–H vibrations), and 3025 cm^{-1} (aromatic C–H vibrations).

At the lower levels of surface coverage produced by the adsorption deposition method, the characteristic PS peaks are difficult to detect by FTIR. However STM

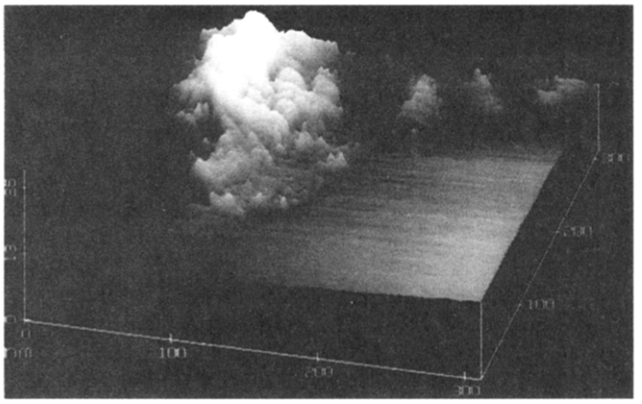

Figure 1. STM image of a discontinuous polystyrene film (M = 18 100) deposited on a HOPG surface by the droplet evaporation method.

images of samples prepared by adsorption revealed surface structures similar to the amorphous clusters produced by droplet evaporation. Figure 2a shows irregularly-shaped "micro-islands" produced by adsorption of M = 18 100 PS on HOPG. In comparison with the discontinuous film formed by droplet evaporation in Figure 1, the micro-islands shown in Figure 2a have similar morphologies but are more isolated and much smaller in size. As a control, several HOPG substrates treated with pure HPLC grade toluene (no polymer) were also imaged. Surface irregularities such as graphite flakes and steps were present on the toluene-treated surfaces, but few foreign particles were observed. Other studies[14] have reported that "ultrasmall" particles with diameters of 0.5−1 nm have also been found on graphite surfaces, but we did not observe these particles on our specimens. The rounded, irregular shapes of the micro-islands are easily distinguishable from graphite steps and flakes, which generally exhibit angular edges and flat tops. Moreover, the micro-islands were only present on the substrates exposed to PS solutions.

Additional evidence that the micro-islands are adsorbed PS comes from scanning tunneling spectroscopy (STS), which yielded similar spectra for both the discontinuous PS films deposited by solution evaporation and the adsorbed micro-islands. Measurements of d(ln I)/d(ln V) were performed over surface areas covered by micro-islands and over polymer-free HOPG surfaces. The micro-islands exhibited d(ln I)/d(ln V) curves distinctly different from those observed for polymer-free HOPG surfaces, including surfaces where graphite flakes and steps were present. While STS measurements proved useful in distinguishing the micro-islands from surface artifacts, the resolution and reproducibility of this method were not sufficient to identify a fingerprint spectrum for PS. Finally, very persuasive evidence that the imaged micro-island structures are PS comes from the direct correlation of micro-island volume with the adsorbate molecular weight, as discussed below.

Adsorbed PS Micro-Island Structures. The micro-island structures shown in Figure 2a for M = 18 100 are characteristic of the surface structures produced by adsorption for all the PS molecular weights studied. Figure 2b−d shows typical micro-island structures for other molecular weights. While the sizes of these structures increase with molecular weight, their shapes are similar.

At the low surface coverages of our adsorption experiments, the adsorbed structures are composed of a relatively small number of polymer molecules, and some structures are individual polymer molecules. The micro-islands imaged in Figure 2a−d are the collapsed structures remaining after the solvent is evaporated from adsorbed polymer structures, thus the imaged shapes represent the "footprints" of the original structures adsorbed from solution. Under these conditions, the dimensions of the micro-islands should vary directly with the molecular weight of the adsorbate. The use of monodisperse PS standards in this study provides an opportunity to investigate this relationship. Both the dimensions of the micro-islands and their degree of aggregation (i.e. the number of molecules contained within each adsorbed structure) can provide important information about the adsorption process.

For each PS molecular weight, several (up to 20) HOPG substrates were prepared by PS adsorption to provide a representative ensemble of adsorbed polymer structures for STM imaging. Graphite substrates treated with adsorbed PS were imaged in a series of 1000 nm × 1000 nm windows using scanner A. Upon completion of scanning a particular 1000 nm × 1000 nm window, the scanning area was changed and imaging was resumed in a new 1000 nm × 1000 nm area. The bias voltage and gain were adjusted for each scanning window to provide stable, high-contrast images, while the tunneling current was usually fixed at 0.3 nA. Usually, these adjustment produced high-quality images of the surface and the adsorbed polymer structures; however in a few surface regions stable images could not be obtained. Polymer structures were not evaluated in these unstable scanning regions. Each 1000 nm × 1000 nm window was further subdivided by zooming into smaller areas to provide higher definition of polymer structures, and the surface features found within each scanning window were examined carefully to distinguish polymer structures from artifacts such as graphite flakes. The images of all structures identified as polymers were captured and retained for later analysis. This scanning procedure was repeated for a number of windows to accumulate a reasonably large ensemble (usually about 100) of polymer images for each PS molecular weight.

The dimensions of the captured polymer images were evaluated by mapping a grid into each imaged structure, as shown in Figure 3. The grid is aligned so that the x axis of the grid coincides with the principal axis of the imaged polymer structure in a 2-dimensional view. The average length $\langle x \rangle = \sum l_i/n$ along the principal axis and the average length $\langle y \rangle = \sum w_j/m$ along the minor axis are evaluated from measurements of the structure's dimensions on an n X m grid, where the grid increments n and m typically divide the major and minor axes into at least five intervals. The surface area A of the structure was evaluated by $A = \Delta y \sum l_i = \Delta x \sum w_j$, where Δx and Δy are the distances between adjacent grid lines in the x and y directions. From the area A, we can determine the equivalent radius of the structure, $R = (A/\pi)^{1/2}$. The cumulative area covered by all the polymers found on the surface is used to compute the surface coverage.

The thickness of the micro-islands is not evident from two-dimensional images such as Figure 2; however STM is inherently a profilometry technique, and data from the scans may be used to evaluate the thickness of the structure. The average thickness t is determined from the thicknesses t_{ij} measured at each grid point: $t = \sum t_{ij}/nm$. In STM imaging of conducting surfaces of

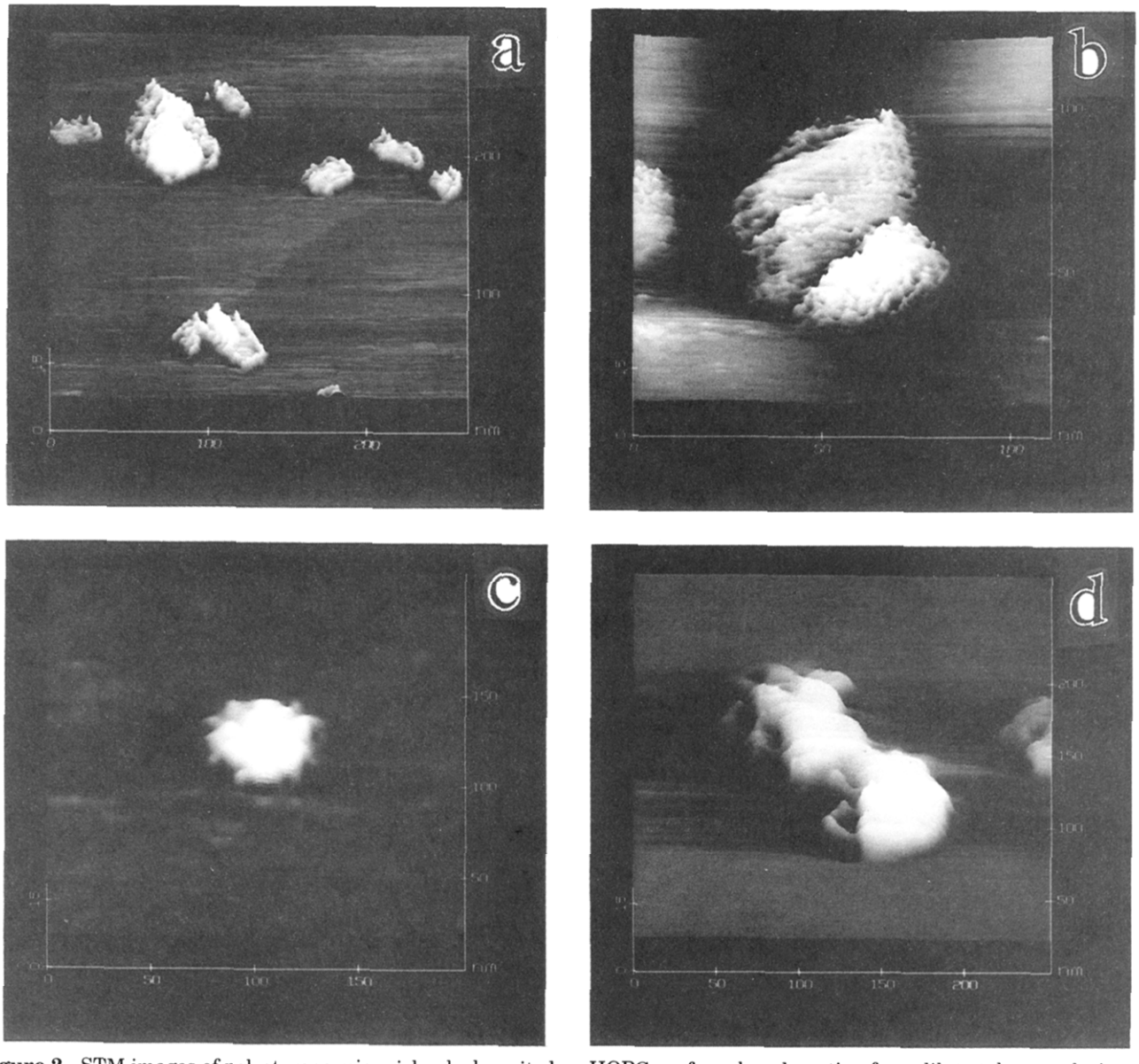

Figure 2. STM images of polystyrene micro-islands deposited on HOPG surfaces by adsorption from dilute toluene solutions of different molecular weight polystyrene solutes: (a) M = 18 100; (b) M = 106 280; (c) M = 707 000; (d) M = 3 000 000.

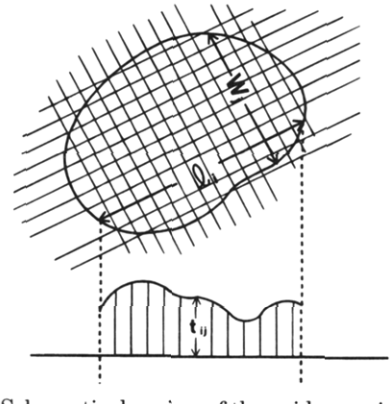

Figure 3. Schematic drawing of the grid mapping technique used to evaluate the dimensions of imaged PS micro-islands.

uniform chemical composition, these thickness values would be interpreted as absolute measures of the thicknesses of surface features. However the STM contrast mechanism for nonconducting organic layers such as our adsorbed PS structures is not well understood, therefore the thicknesses measured by STM may not be absolute. If electron tunneling is the predominant contrast mechanism, as in STM imaging of conductive surfaces, one might expect the measured thicknesses to be influenced by changes in the local density of states (LDOS) as the tip moves from regions of pure graphite to regions covered by the nonconducting polymer. On the other hand, Yuan et al.[25] have proposed a nontunneling contrast mechanism for nonconducting specimens wherein the STM tip is presumed to be in direct contact with a condensed layer of water on the surface that acts as an ionic conductor, thereby establishing the current flow. According to this mechanism, the tip follows the surface profile, maintaining electrical contact with the water film, provided the water film is continuous and relatively uniform in thickness, thereby yielding absolute thickness measurements. Our experiments do not yield sufficient information to discern among these and other possible contrast mechanisms,[26] therefore we interpret our thicknesses with some caution as relative, but not necessarily absolute, measurements of the true thickness of the adsorbed polymer structures. This interpretation is reinforced by limited comparisons of thicknesses of adsorbed PS structures measured directly by STM (without conductive coatings)

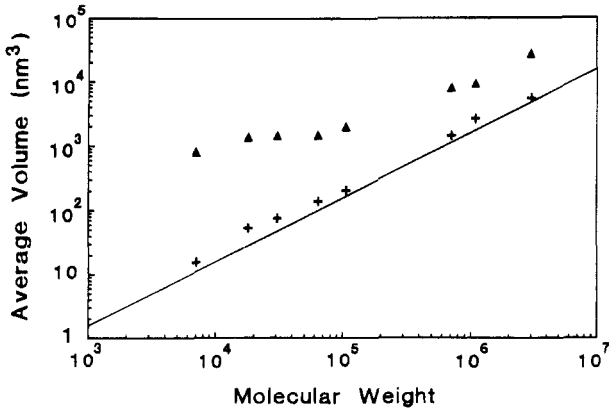

Figure 4. Variation of micro-island volume with molecular weight. The straight line represents the molecular volume of polystyrene calculated from the bulk density (1.05 g/cm^3). Symbols: (▲) number average volume of micro-islands for each molecular weight; (+) average volume of the ten smallest micro-islands found for each molecular weight.

to thickness values obtained by performing both STM and AFM imaging on the same specimens after overcoating the surface with a sputtered Au–Pd layer. In two-dimensional views, the dimensions of adsorbed PS structures measured by uncoated STM are in close agreement with those measured by STM and AFM after the coating was applied. The thicknesses measured by the coated STM and coated AFM techniques are in close agreement, and both methods give thicknesses that are about 50% larger than those measured by uncoated STM, thereby confirming the magnitude of the uncoated STM thickness measurements.

Another concern in interpreting the thickness measurements is the possibility that a soft organic layer can be deformed by the tip during scanning. We do not believe that images of our polystyrene structures suffered severe deformation by the tip because (1) the shapes of the imaged polystyrene structures were found to be stable for up to five repeated scans, whereas progressive changes in shape would be expected if high tip deformations were prevalent; (2) the uncoated thickness values were similar in magnitude to the thicknesses measured by STM and AFM on specimens treated with a metallic coating, as described above; and (3) an analysis of the orientation of the principal axis of polymer structures, which is fully described in a later section, did not reveal any preferential orientation of the adsorbed polymers with respect to the direction of scanning, which would likely occur if the polymer was highly deformed by the tip. Nevertheless, some moderate deformation of the PS structures may have occurred during scanning, and possibly this is the reason the thicknesses measured by uncoated STM are consistently smaller than those measured by STM and AFM after metallic overcoating.

The size of micro-islands deposited by the adsorption method was investigated by determining the number-average volume of the imaged micro-islands for each molecular weight. In Figure 4, these results are compared with the volumes of single polymer molecules, calculated from the bulk density of polystyrene (1.05 g/cm^3).[27] This comparison suggests that a typical micro-island is composed of 3–50 individual chains. In view of the unentangled nature of the original solutions and the low surface coverage of the adsorbed PS, this level of aggregation seems surprisingly high. The average number of chains per micro-island appears to decrease

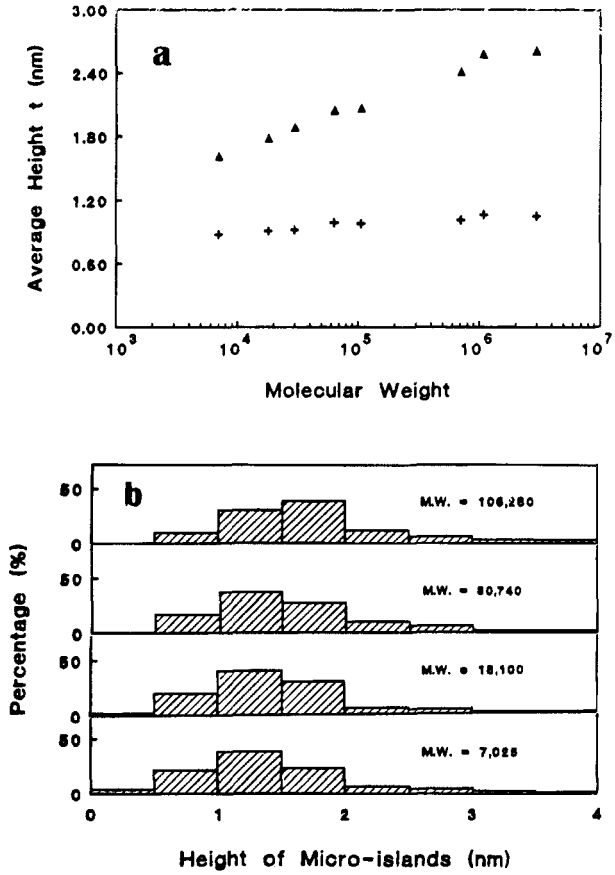

Figure 5. (a) Variation of micro-island thickness with molecular weight: (▲) number-average thickness of micro-islands for each molecular weight; (+) average thickness of the ten smallest micro-islands found for each molecular weight. (b) Distribution of micro-island thicknesses for four polystyrene samples.

with molecular weight. We note, however, that the 1000 nm × 1000 nm scanning area of the STM head used for these measurements may have limited our ability to detect larger structures (possibly present on high-M samples) that span two or more scanning windows.

The second set of points shown in Figure 4 represents the average volumes of the ten smallest micro-islands found for each molecular weight. These values are close to the molecular volumes calculated from the bulk density, suggesting that many of these small micro-islands contain only a single polymer chain. Stange *et al.*[11] have reported similar volumes for PS structures produced by spin coating of 0.0005 wt % PS solutions onto silicon wafers, and they also concluded that the smallest observed structures were single PS chains. As discussed above, the direct correlation of the average volume of the smallest micro-islands with adsorbate molecular weight provides strong evidence identifying these structures as polystyrene.

Figure 5a shows the variation of number-average micro-island thickness with molecular weight and the corresponding thickness of the 10 smallest structures for each M. The overall number-average thickness increases as a weak function of molecular weight, with thickness increasing by only a factor of 2 over nearly three decades of M. The thickness of the smallest structures (single chains) is nearly independent of M. Figure 5b shows details of the distribution of measured micro-island thicknesses for four of the PS adsorbates studied. These distribution plots are very similar, following a roughly Gaussian distribution about the

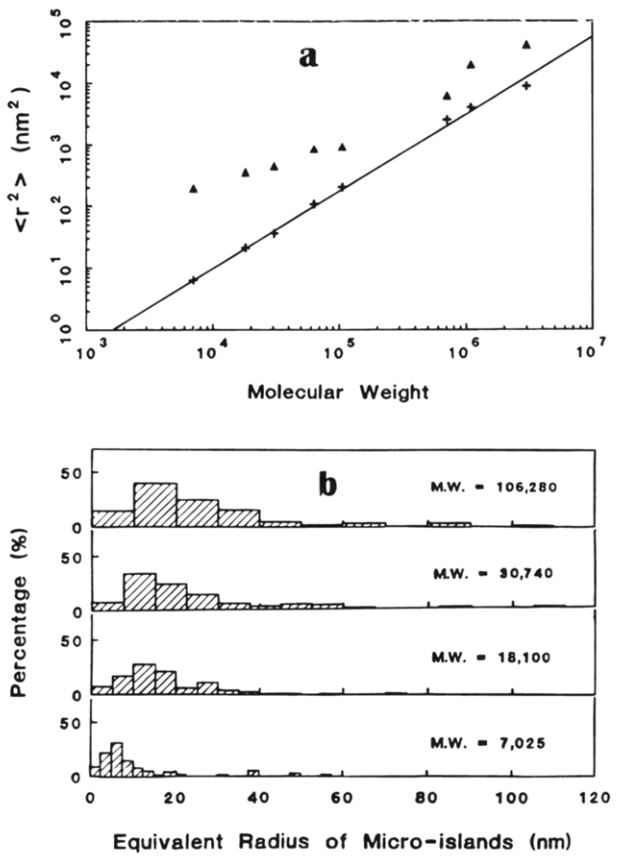

Figure 6. Variation of mean square radius of micro-islands with molecular weight: (▲) overall mean square radius of micro-islands for each molecular weight; (+) mean square radius of the ten smallest micro-ligands found for each molecular weight. The solid line represents the linear regression fit yielding $\langle r^2 \rangle \propto M^{1.24}$. (b) Distribution of micro-island radii for four polystyrene samples.

mean thickness values. The mean thickness for each curve is in the range 1.5−3 nm, which is comparable to the spin-cast film thicknesses observed by Stange *et al.*[11] at low PS concentrations (0.075−0.1 wt %). The weak dependence of apparent thickness on M is consistent with theoretical predictions for adsorption of isolated polymer chains on interacting surfaces from good solvents (e.g. the Brownian dynamics simulations of Bishop and Clarke[1]).

Figure 6a shows that the mean square radius $\langle r^2 \rangle$ of the PS micro-islands increases directly with molecular weight. A second set of points represents data for the ten smallest structures for each M. In Figure 6b, the distribution of micro-island radii about the mean value is shown for four values of M corresponding to those displayed in Figure 5b. Again, Gaussian-shaped distributions about the mean values are observed. A comparison of the mean square radii $\langle r^2 \rangle$ to the mean square thicknesses $\langle t^2 \rangle$ shows that the adsorbed micro-islands are thin structures, with $\langle r^2 \rangle / \langle t^2 \rangle$ varying from 25 to 600. This finding is consistent with the train-and-loop model[28] for polymer adsorption from good solvents onto interacting surfaces,[29−32] and with simulation results for single chains.[1−3] The large $\langle r^2 \rangle / \langle t^2 \rangle$ ratios observed here are also promoted by the collapse of the adsorbed polymers onto the surface as the solvent is removed. Loops of the polymer chain that may have originally protruded into the solvent cannot be discerned in these images. What is seen after solvent evaporation is a collapsed "footprint" of the original adsorbed polymer conformation.

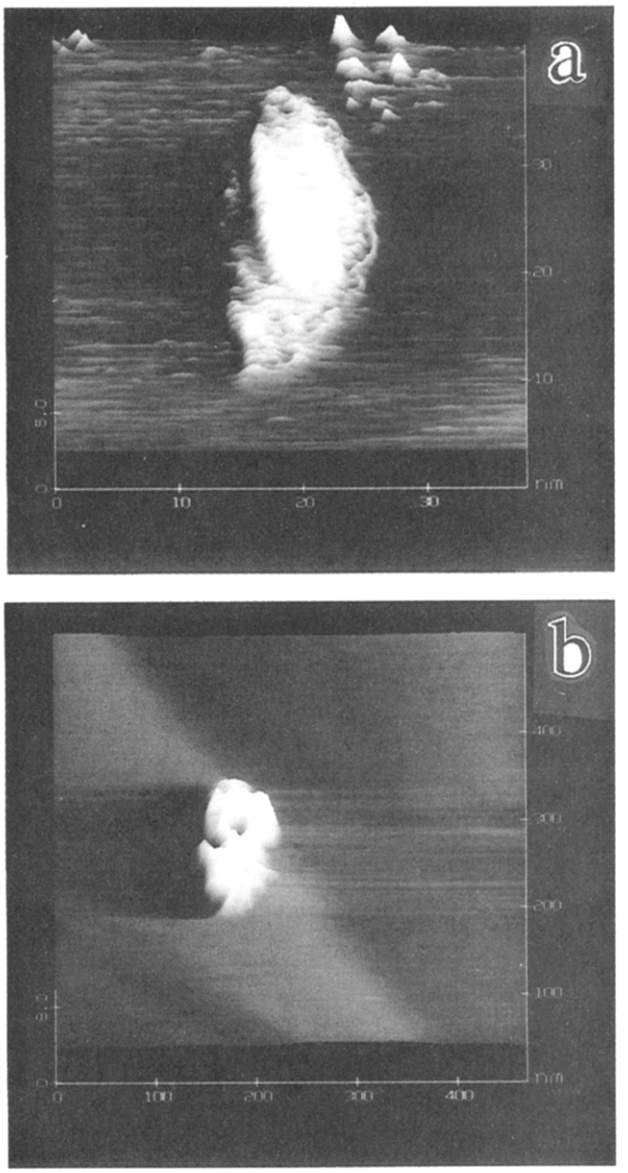

Figure 7. STM images of small polymer micro-islands for two molecular weights: (a) M = 30 740; (b) M = 3 000 000. The volumes of these structures are comparable to the molecular volume of PS (see Figure 4), which suggests that they are single polystyrene chains.

The solid line through the points in Figure 6a representing the ten smallest micro-islands observed at each molecular weight has a slope of 1.24, indicating that $\langle r^2 \rangle$ scales with $M^{1.24}$. This exponent is consistent with the scaling relationship[33] $\langle S^2 \rangle \propto M^{1.2}$ for polymers dissolved in good solvents, where $\langle S^2 \rangle$ is the mean square radius of gyration. The observed scaling of $\langle r^2 \rangle$ with $M^{1.24}$ also compares closely with the Brownian dynamics simulations of Bishop and Clarke,[1] which show the component of the mean square radius of gyration parallel to the surface scales with M raised to an exponent near 1.2 for polymer chains adsorbed from good solvents onto surfaces with low to moderately attractive polymer−surface interaction potentials (up to about $\epsilon_{BS} = 0.5$ in the dimensionless interaction potential used in ref 1). The observed scaling exponent of 1.24 is markedly higher than the scaling exponents predicted for polymer adsorption from poor solvents onto moderately interacting surfaces, which are near 1.0 and 0.7, respectively, for Θ solvents and nonsolvents that produce chain collapse. The experimental exponent is also distinctly lower than the predicted scaling exponent

Table 3. Ratio of Mean Square Minor Axis Length to Mean Square Major Axis Length, $\langle y^2\rangle/\langle x^2\rangle$, and the Angle, θ, of Principal Axis Relative to the Scanning Direction

molecular weight	$\langle y^2\rangle/\langle x^2\rangle^{a,b}$ for PS micro-islands	$\langle y^2\rangle/\langle x^2\rangle^{a,b}$ for single molecules	$\langle \cos^2\theta\rangle^a$ for PS micro-islands	$\langle \cos^2\theta\rangle^a$ for single molecules
7 025	0.595(0.332) (165)	0.634(0.210) (12)	0.484(0.31)	0.472(0.30)
18 100	0.621(0.326) (178)	0.543(0.140) (14)	0.509(0.33)	0.480(0.31)
30 740	0.576(0.355) (163)	0.542(0.168) (13)	0.488(0.32)	0.491(0.29)
64 000	0.611(0.329) (122)	0.551(0.164) (12)	0.472(0.30)	0.502(0.30)
106 280	0.512(0.310) (148)	0.514(0.138) (14)	0.491(0.30)	0.452(0.31)
707 000	0.564(0.343) (106)	0.532(0.153) (10)	0.514(0.31)	0.489(0.28)
1 090 000	0.588(0.318) (98)	0.507(0.188) (12)	0.486(0.33)	0.503(0.32)
3 000 000	0.623(0.351) (76)	0.558(0.170) (11)	0.507(0.34)	0.488(0.30)
all samples	0.586(0.333) (1056)	0.547(0.167) (98)	0.494(0.32)	0.485(0.30)

[a] Standard deviation (in first set of parentheses). [b] Total number of clusters analyzed (in second set of parentheses).

of 1.5 for adsorption from good solvents onto very strongly attractive surfaces. Since toluene is a good solvent for polystyrene and HOPG is not a strongly attractive surface, the experimental scaling exponent determined from Figure 6a seems to be in excellent agreement with theory.

Adsorbed PS Molecules. The comparison of micro-island volumes to the calculated volumes of PS chains shown in Figure 4 suggests that the smallest of the micro-islands are single polymer molecules. Images of these small single-chain structures, displayed for two molecular weights in Figure 7a,b, show the same rounded contours as the larger micro-islands. In two-dimensional views such as in Figure 7, these structures are usually elongated in shape rather than circular. This finding is in qualitative agreement with the 3-dimensional conformational simulations of Solc and Stockmayer[34] and the 2-dimensional simulations of Solc and Gobush,[35] which show that typical polymer conformations are elongated rather than spherical (3-D) or circular (2-D).

The dimensions of single adsorbed molecules were analyzed by the grid mapping procedure described earlier to evaluate the lengths of the major (x) and minor (y) axes, and the angle formed between the major axis and the scanning direction. To develop statistically significant averages, roughly 100 molecular-size images of adsorbed polymers were analyzed, as detailed in Table 3. The deviation of the shapes of individual adsorbed polymer molecules from the "average" circular shape is evident from the ratios of mean square minor axis length to mean square major axis length $\langle y^2\rangle/\langle x^2\rangle$, which range from 0.51 to 0.62 for micro-islands of all sizes, and from 0.51 to 0.63 for the smallest (single-chain) micro-islands. Since an adsorbed polymer structure occupying a circular area of surface would have $\langle y^2\rangle/\langle x^2\rangle = 1$, the adsorbed structures in our study are clearly elongated rather than circular. Moreover, the shape does not appear to depend on either molecular weight or the degree of aggregation. Quantitatively, these data cannot be readily compared with chain statistics derived from simulations of polymers in solution (e.g. Solc and Stockmayer[34] and Solc and Gobush[35]) because the images represent collapsed adsorbed structures rather than free chains. However the data provide direct information about adsorbed polymer conformations, and a complementary theoretical investigation would be quite useful.

The angle of principal axis relative to the scanning direction θ is also of interest, because it can reveal whether any orientation effects have been introduced by the scanning process. For the case of randomly distributed orientations, the mean square cosine of the orientation angle $\langle \cos^2\theta\rangle$ is equal to 0.5 and has a standard deviation of 0.354. Values for $\langle \cos^2\theta\rangle$ from our imaging experiments, given in Table 3, vary from 0.47 to 0.51, with no discernable dependence on molecular weight or micro-island size. For the 1056 structures imaged to compile Table 3, the average value for $\langle \cos^2\theta\rangle$ is 0.494 and the standard deviation is 0.32. These experimental values are very close to the theoretical values for a random distribution, indicating that the effect of scanning on the orientation of the imaged structures is negligible for the scanning conditions employed here. We also note that there is no preferred alignment of the PS micro-islands with respect to the crystallographic axes of the HOPG substrates. Since no influence of scanning on the orientation angle is evident, we can infer that the dimensions of the imaged structures are largely unaffected by scanning under the conditions used here.

Conclusions

This study demonstrates that the topologies of polystyrene micro-islands adsorbed on HOPG substrates from dilute polymer solutions can be directly imaged by STM without the use of conductive overcoating. The micro-islands are the thin, flat, collapsed structures of strongly adsorbed polystyrene molecules that remain on the surface after solvent evaporation. The mean square radius of the micro-islands varies directly with molecular weight, but the average thickness increases only weakly with M. The number-average micro-island volumes range from 3 to 50 times the volumes of individual polymer molecules, with the greatest aggregation observed at the lowest molecular weight.

The volumes of the smallest micro-islands imaged at each molecular weight were close to the molecular volumes calculated from the bulk density of polystyrene, suggesting that these structures are individual polymer chains. Like the larger micro-islands, the individual chains were thin, flat structures, and the thickness was found to be nearly independent of molecular weight. The mean square radius of the individual chains was found to vary with $M^{1.24}$, which is in close agreement with theoretical predictions for polymers adsorbed from good solvents onto moderately attractive surfaces. The dimensions of the major axis (x) and minor axis (y) in two dimensions were evaluated for each of the individual chain images, and the typical "footprint" of an adsorbed PS molecule was found to be elongated, with $\langle y^2\rangle/\langle x^2\rangle = 0.55$, rather than circular. Thus the STM images provide direct evidence of the asymmetric conformations of random-coil polymers predicted by statistical theories.[34,35]

The angle θ between the major axis and the scanning direction was also analyzed to identify any possible distortion of the chains due to scanning. Both the mean

and standard deviation of the quantity $\langle \cos^2 \theta \rangle$, calculated from data for 1056 micro-islands and individual chains, were found to be consistent with a random distribution of θ. Therefore we conclude that STM scanning induces little, if any, orientation or distortion of the polymer structures under the conditions of these experiments. This finding, together with the generally satisfactory correlation of the sizes of imaged molecules with those calculated from the bulk density of PS, confirms that direct STM imaging, without conductive overcoating, is a useful technique for conformational study of amorphous, nonconducting polymers.

Acknowledgment. The authors are grateful to Dr. F. T. Wagner and to the Physical Chemistry Department of General Motors Research and Development Center for the use of their STM facilities for the experiments reported here.

References and Notes

(1) Bishop, M.; Clarke, J. H. R. *J. Chem. Phys.* **1990**, *93*, 1455.
(2) Balazs, A. C.; Huang, K.; McElwain, P.; Brady, J. E. *Macromolecules* **1991**, *24*, 714.
(3) Kumbar, M.; Windwer, S. *J. Chem. Phys.* **1968**, *49*, 4057.
(4) Fleer, G. J.; Lyklema, J. In *Adsorption from Solution at the Solid/Liquid Interface*; Parfitt, G. D., Rochester, C. H., Eds.; Academic Press Inc.: London, 1983; Chapter 4.
(5) Howard, G. J. In *Interfacial Phenomena in Apolar Media*; Eicke, H.-F., Parfitt, G. D., Eds.; Marcel Dekker, Inc.: New York, 1987; Chapter 7.
(6) Richardson, M. J. *Proc. R. Soc. London, Ser. A* **1964**, *279*, 50.
(7) Quayle, D. V. *J. R. Microsc. Soc.* **1967**, *87*, 353.
(8) Furuta, M. *J. Polym. Sci., Polym. Phys. Ed.* **1976**, *14*, 479.
(9) Williams, R. C.; Wyckoff, R. W. G. *J. Appl. Phys.* **1944**, *15*, 712.
(10) Binnig, G.; Rohrer, H. *IBM J. Res. Dev.* **1986**, *30*, 355.
(11) Stange, T. G.; Mathew, R.; Evans, D. F.; Hendrickson, W. A. *Langmuir* **1992**, *8*, 920.
(12) Salmeron, M.; Beebe, T.; Odriozola, J.; Wilson, T.; Ogletree, D. F.; Siekhaus, W. *J. Vac. Sci. Technol. A* **1990**, *8*, 635.
(13) Clemmer, C. R.; Beebe, T. P., Jr. *Science* **1991**, *251*, 640.
(14) Chang, H.; Bard, A. J. *Langmuir* **1991**, *7*, 1143.
(15) Hobden, J. F.; Jellinek, H. H. *J. Polym. Sci.* **1953**, *11*, 365.
(16) Einaga, Y.; Miyari, Y.; Fujita, H. *J. Polym. Sci., Phys. Ed.* **1979**, *17*, 2103.
(17) Albrecht, T. R.; Dovek, M. M.; Lang, C. A.; Grutter, P.; Quate, C. F.; Kuan, S. W. J.; Frank, C. W.; Pease, R. F. W. *J. Appl. Phys.* **1988**, *64*, 1178.
(18) Fujiwara, I.; Ishimoto, C.; Seto, J. *J. Vac. Sci. Technol. B* **1991**, *9*, 1148.
(19) Moiseev, Y.; Panov, V.; Savinov, S.; Yaminsky, I.; Todua, P.; Znamensky, D. *Ultramicroscopy* **1992**, *42–44*, 304.
(20) Wilson, T. E.; Ogletree, D. F.; Salmeron, M. B.; Bednarski, M. D. *Langmuir* **1992**, *8*, 2588.
(21) Sano, M.; Sasaki, D. Y.; Kunitake, T. *Macromolecules* **1992**, *25*, 6961.
(22) Hawley, M. E.; Benicewicz, B. C. *J. Vac. Sci. Technol. B* **1991**, *9*, 1141.
(23) Yang, R.; Yang, X. R.; Evans, D. F.; Hendrickson, W. A.; Baker, J. *J. Phys. Chem.* **1990**, *94*, 6123.
(24) Dibbs, M. G. In *Encyclopedia of Polymer Science and Engineering*; John Wiley and Sons: New York, 1989; Vol. 16, p 152.
(25) Yuan, J.-Y.; Shao, Z.; Gao, C. *Phys. Rev. Lett.* **1991**, *67*, 863; *Phys. Rev. Lett.* **1992**, *68*, 2563.
(26) Hörber, J. K. H.; Häberle, W.; Ruppersberg, P.; Smith, D. P. E.; Binnig, G. *J. Vac. Sci. Technol. B* **1994**, *12*, 2243.
(27) Rodriguez, F. *Principles of Polymer Systems*; Hemisphere Publishing Co.: New York, 1989; Appendix 5.
(28) Jenkel, E.; Rumbach, B. *Z. Elektrochem.* **1951**, *55*, 612.
(29) Hoeve, C. A. J. *J. Polym. Sci., Part C* **1971**, *34*, 1.
(30) Silberberg, A. *J. Chem. Phys.* **1968**, *48*, 2835.
(31) Roe, R. J. *J. Chem. Phys.* **1974**, *60*, 4192.
(32) Scheutjens, J. M. H. M.; Fleer, G. J. *J. Phys. Chem.* **1980**, *84*, 178.
(33) de Gennes, P.-G.; *Scaling Concepts in Polymer Physics*; Cornell University Press: Ithaca, NY, 1979.
(34) Solc, K.; Stockmayer, W. H. *J. Chem. Phys.* **1971**, *54*, 2756.
(35) Solc, K.; Gobush, W. *Macromolecules* **1974**, *7*, 814.

MA9503569